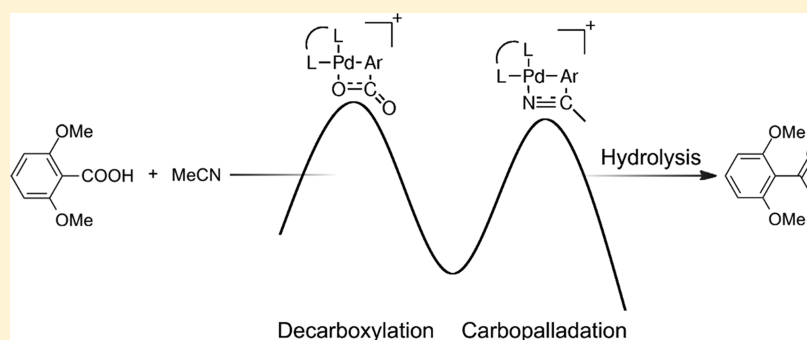


Theoretical and Experimental Investigation of Palladium(II)-Catalyzed Decarboxylative Addition of Arenecarboxylic Acid to Nitrile

Fredrik Svensson, Rajendra S. Mane, Jonas Sävmarker, Mats Larhed, and Christian Sköld*

Organic Pharmaceutical Chemistry, Department of Medicinal Chemistry, BMC, Uppsala University, P.O. Box 574, SE-751 23 Uppsala, Sweden

S Supporting Information



ABSTRACT: The reaction mechanism of palladium(II)-catalyzed decarboxylative addition of 2,6-dimethoxybenzoic acid to acetonitrile was investigated by means of density functional theory (DFT) calculations. Calculations of the free energy profile for decarboxylation and carbopalladation indicated carbopalladation as the rate-determining step of the reaction. Investigation of the free energy profile for a series of experimentally evaluated nitrogen-based bidentate palladium ligands revealed that higher energy is required for decarboxylation and carbopalladation employing the experimentally least efficient ligand. The DFT investigation also showed that the relative free energies of the transition states were lowered in polar solvent, and preparative experiments confirmed that a nonoptimal ligand could be greatly improved by addition of water to the reaction system.

INTRODUCTION

Ketone moieties are common structural features in pharmaceuticals and natural products. There are a number of different methods to produce ketones, and one elegant way of producing aryl ketones is the carbon–transition metal 1,2-carbopalladation of a nitrile moiety followed by hydrolysis of the formed ketimine. Although this method was first reported in 1970,¹ it has recently received increased attention with the development of protocols employing palladium catalysis by Larock and co-workers.^{2,3} Several efficient protocols for synthesizing aryl ketones via an initial C–H activation,^{2,3} oxidative addition,^{4,5} transmetalation,^{6–8} decarboxylation,⁹ or desulfination^{10–12} are now available.

Catalytic decarboxylation of benzoic acid analogues provides a highly interesting transformation that utilizes cheap and available carboxylic acids as aryl sources.¹³ Decarboxylation of benzoic acid and substituted benzoic acids is well known for uncatalyzed systems¹⁴ and has also been explored for Cu,^{15,16} Pd,¹⁷ Ag,¹⁸ Au,¹⁹ Rh,²⁰ and mixed Pd/Cu catalysis.^{21–25} Larhed and co-workers utilized Pd(II)-catalyzed decarboxylation of benzoic acid analogues in order to generate the active Pd–aryl intermediate that precedes carbopalladation.⁹ Mechanistic investigations of decarboxylation using DFT calculations have been performed for metal-catalyzed systems employing Pd,^{26,27}

Cu,^{16,18,28} and Ag,¹⁸ as well as for uncatalyzed systems.^{29–33} In contrast, to the best of our knowledge no theoretical mechanistic investigations of the formation of the ketimine have been published.

The focus of this study is the Pd(II)-catalyzed decarboxylative addition of 2,6-dimethoxybenzoic acid (**1**) to acetonitrile (MeCN) as reported by Lindh et al. (Scheme 1), which has been used as a model reaction for the development of optimal reaction conditions to produce aryl ketones.⁹ Lindh et al. investigated the reaction by means of electrospray ionization mass spectrometry (ESI/MS) to characterize intermediate palladium complexes, and on the basis of mechanistic studies, the reaction is believed to proceed by an initial decarboxylation of **1**, producing a Pd–aryl species and subsequent carbopalladation of MeCN to form the ketimine **2**. The ketimine is readily hydrolyzed to form the corresponding ketone **3**, with the exception of sterically hindered mesityl ketimines.^{3,9}

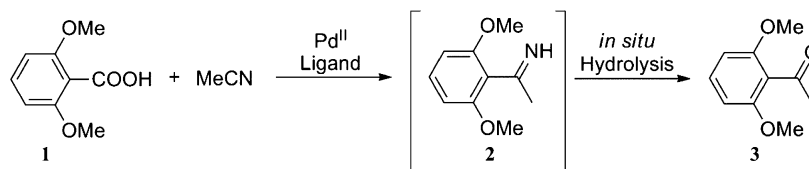
The efficiency of the Pd(II)-catalyzed addition reaction was strongly affected by the ligand used. Within a series of related nitrogen-based bidentate ligands L1–L7 (Table 1) the yields ranged from 16 to 73% under the same reaction conditions. In

Received: October 11, 2012

Published: January 11, 2013



Scheme 1. Reaction Scheme

Table 1. Nitrogen Ligands and Isolated Yields of 3 from 1 and MeCN (Scheme 1) As Reported by Lindh et al.⁹

Ligand	Structure	Yield [%] ^a
L1		16
L2		32
L3		73 63 ^b
L4		36
L5		18
L6		68
L7		67

^aIsolated yields. ^bPd(OAc)₂ was used instead of Pd(O₂CCF₃)₂.

general the methyl-substituted bipyridines or phenanthrolines L3, L4, L6, and L7 were more efficient ligands in the reaction in comparison to the nonsubstituted analogues L1, L2, and L5. The beneficial effect from the methyl groups in phenanthrolines and corresponding bipyridines could possibly be attributed to destabilization of square-planar complexes in the reaction pathway.³⁴

Mechanistic studies of the reaction may provide valuable insights into the catalytic system and aid in the development of improved protocols. Herein we investigate the two main reaction steps, i.e., decarboxylation and carbopalladation, by means of DFT calculations and explore the effect of ligands and solvents on the energy profile of the reaction.

EXPERIMENTAL DETAILS

Computational Details. All DFT calculations were carried out using Jaguar³⁵ version 7.8 employing the B3LYP hybrid functional^{36–38} and LACVP* basis set, which uses an effective core potential for Pd and 6-31G* for elements H–Ar.³⁹ The B3LYP functional has for many years been the most widely used density functional⁴⁰ and has been used together with variants of the 6-31G basis set for examining reaction profiles of Pd(II)-catalyzed decarboxylation and carbopalladation.^{27,41,42} The complexes were optimized in the gas phase, and the optimized structures were subsequently subjected to a single-point energy calculation using the

PBF solvation model with default settings in Jaguar for water or acetonitrile where applicable.^{43,44} Dispersion correction was calculated using the DFT-D3 program.⁴⁵ Frequencies and thermodynamic contribution to the free energy were calculated for the optimized geometries in the gas phase at 373.15 K. The reported free energies were calculated by adding the thermodynamic correction, including zero-point energy, and the dispersion correction to the single-point solution phase energy.

The presented transition states (TSs) were verified to have only one imaginary frequency and were verified to be connected to the presented succeeding and preceding energy minima, respectively. All stationary minima were verified to have no imaginary frequencies.

Figures 2 and 4 were prepared using XYZ-viewer.⁴⁶

Chemistry. Reaction Conditions for Ligand Investigation (Table 1) As Reported by Lindh et al.⁹ A 5 mL microwave vial was charged with 2,6-dimethoxybenzoic acid (0.5 mmol), Pd(O₂CCF₃)₂ (0.02 mmol), ligand (0.024 mmol), H₂O (200 μL), and MeCN (2 mL). The vial was capped in air and exposed to microwave heating for 30 min at 130 °C.

Reaction Conditions for Water Content Investigation (Table 3). A 5 mL process vial was charged with 2,6-dimethoxybenzoic acid (91 mg, 0.5 mmol), Pd(O₂CCF₃)₂ (6.6 mg, 0.02 mmol), 2,2'-bipyridine (3.9 mg, 0.025 mmol), H₂O (200–1600 μL), and MeCN (600–2000 μL) in a combination resulting in the same total volume. The vial was capped in air and exposed to microwave heating for 30 min at 130 °C.

RESULTS AND DISCUSSION

The calculations were set up using Pd(OAc)₂ as the palladium source, acetonitrile as the solvent, and reactant and calculating thermochemical properties at 373.15 K, conditions known to yield product. Ligand L3 was chosen as the reference ligand, since it has been reported to give the best yields and we chose to focus our investigation on the reaction path indicated by the reported ESI/MS studies.⁹

The energies for dissociation and association between different complexes considered were not calculated but have been estimated to be diffusion limited with a energy requirement in the magnitude of 20 kJ mol^{−1}.⁴⁷ A dashed line in the free energy profiles indicates that the pathway for the connection was not investigated.

Decarboxylation. The free energy profile for decarboxylation is shown in Figure 1. The starting point for the investigation was the ligated diacetate Pd(II) complex I. Replacement of an acetate with 1 gave complex II (Figure 2), which is 6 kJ mol^{−1} lower in energy and resulted in the lowest energy complex found preceding decarboxylation. This low-energy complex II was chosen as reference, and all other energies are reported relative to this. Palladium(II)-catalyzed decarboxylation of benzoic acid has been investigated by others by means of DFT calculations.^{26,27} In those investigations the decarboxylation TS is higher in energy than any of the complexes preceding the TS. On the basis of those results it is reasonable to assume that this is also the case in our investigation, and because numerous pathways are possible, the specific pathway from II to the decarboxylation TS was not investigated in great detail. Dissociation of the second acetate produced the cationic complex III with deprotonated 1 in a

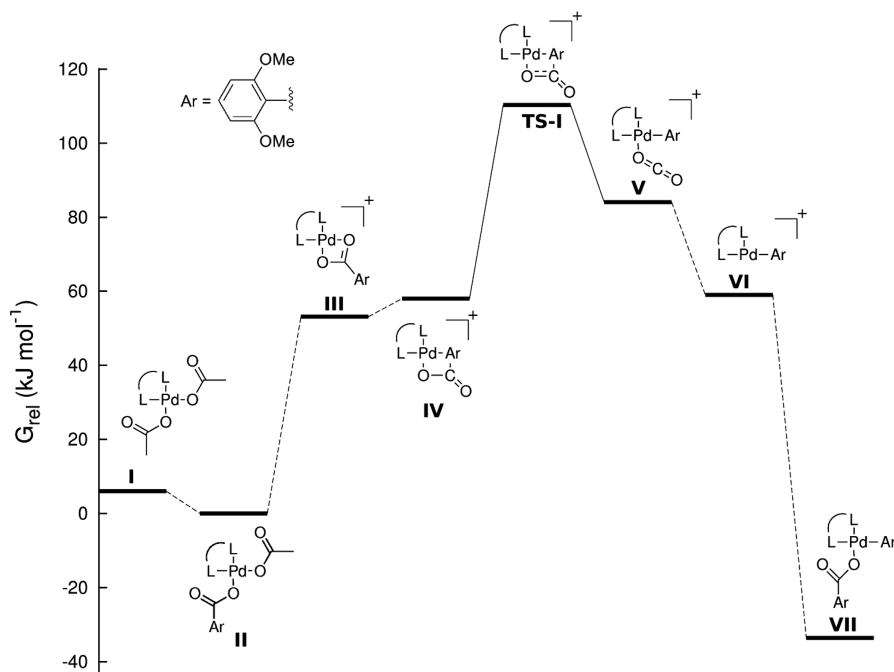
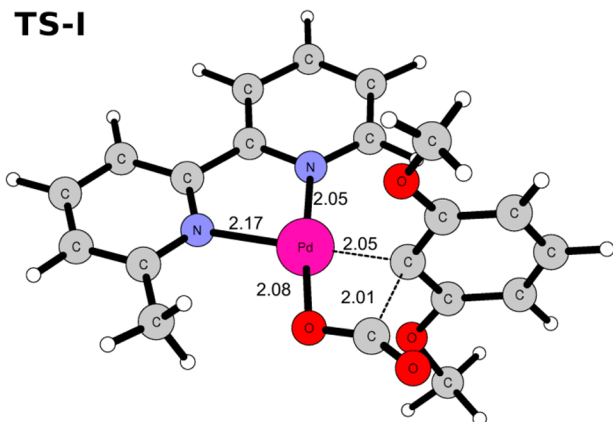


Figure 1. Free energy profile of Pd(II)-catalyzed decarboxylation of **1** using **L3** as ligand.

TS-I



II

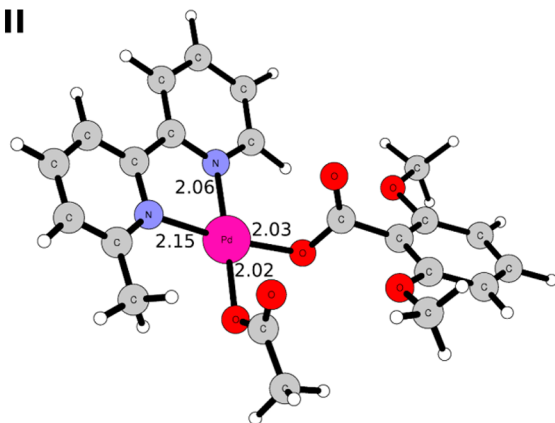


Figure 2. Optimized geometries for **II** and **TS-I**. Bond lengths (Å) between Pd and coordinated atoms and for the breaking carbon–carbon bond in **TS-I** are depicted.

bidentate binding mode, which was the lowest energy minimum found for the cationic predecarboxylation complexes. Changing the binding mode of deprotonated **1** resulted in

complex **IV**, which is connected to **TS-I**, in agreement with previous DFT investigations, which have reported similar TSs and prereactive minima.^{26,27} In **TS-I** (Figure 2) the plane of the carboxylic acid moiety is orthogonal to the plane of the aryl group in **1**. Furthermore, the aryl is located trans to the 6-methyl-substituted pyridine moiety in **L3**, which corresponds to the less sterically hindered pathway. Overall, the free energy required from the preceding lowest energy complex **II** to **TS-I** is calculated to be 110 kJ mol^{−1}, which is similar to that reported for other investigations of Pd(II)-catalyzed decarboxylation of benzoic acid analogues, albeit via neutral TSs.^{26,27} Comparison between neutral and charged complexes and TSs is a challenging task and requires extra care to be taken, since such a comparison is highly dependent on the use of an adequate solvation model.⁴⁸ The continuum solvation model used in this study has been shown to give a fair representation of the relative energies, but solvation of charged molecules is associated with a higher margin of error, which has been estimated for small anions to be in the range of 25 kJ mol^{−1}.⁴⁹ After the decarboxylation product is formed in complex **V**, dissociation of carbon dioxide gave complex **VI**. From **VI** association of acetonitrile formed complex **VIII**, which is ready for carbopalladation of the nitrile. However, in the reaction mixture there are several potential ligands that may give low-energy complexes preceding carbopalladation. It was observed that the neutral complexes were energetically favored and the neutral complex **VII** (Figure 4) was identified as the lowest energy minimum preceding carbopalladation and thus was a suitable starting point for carbopalladation.

Carbopalladation. Figure 3 shows the free energy profile for carbopalladation. Dissociation of deprotonated **1** from complex **VII** followed by association of MeCN gave the cationic precarbopalladation complex **VIII**. In comparison to carbopalladation of alkynes starting from the η^2 binding mode,⁴¹ the η^1 -MeCN approaches the TS by Pd–N–C angle bending up to **TS-II** (Figure 4). This makes the C–N bond, just as in the case with alkynes, parallel to the aryl–Pd bond in

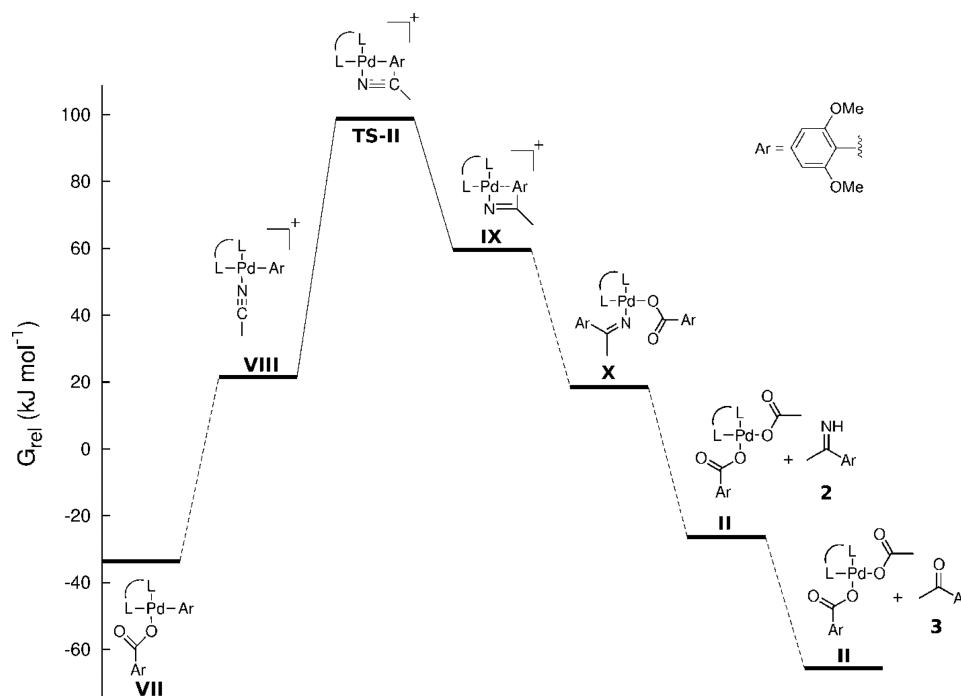


Figure 3. Free energy profile of carbopalladation of MeCN using L3 as ligand.

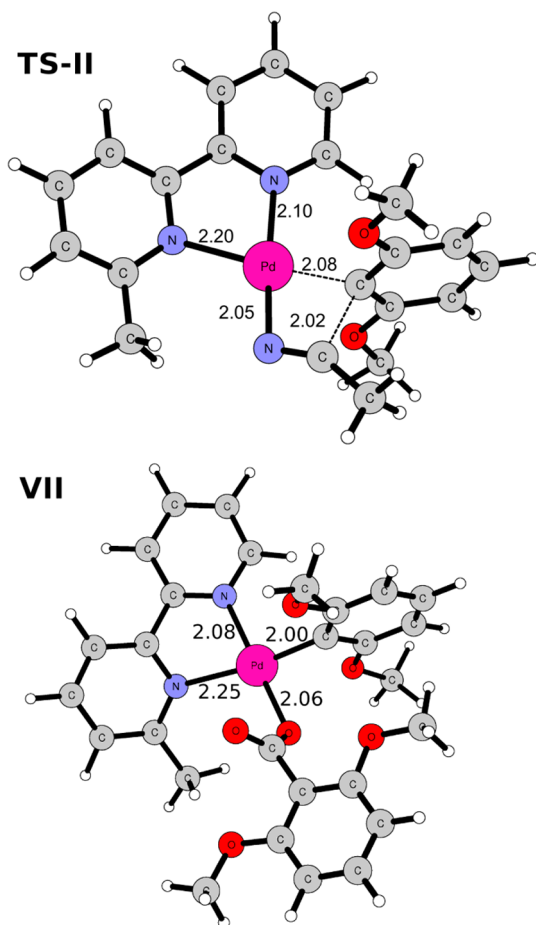


Figure 4. Optimized geometries for VII and TS-II. Bond lengths (Å) between palladium and coordinated atoms and for the forming carbon–carbon bond in TS-II are shown.

the TS and with the plane of the aryl group orthogonal to the plane of the forming ketimine moiety. The energy difference between the carbopalladation TS of the alkyne and the prereactive complex is reported to be 85 kJ mol^{-1} , which is in the same range as the corresponding energy required for carbopalladation of acetonitrile from VIII, which is calculated to be 77 kJ mol^{-1} . The free energy required for the full carbopalladation step starting from VII is calculated to be 132 kJ mol^{-1} .

From TS-II the formation and release of the imine product starts with complex IX. Subsequent association of deprotonated **1** gives the neutral complex X, which is lower in energy. Replacing the carbopalladation product **2** in complex X for acetate regenerates the starting complex II, and hydrolysis yields the target ketone **3**, which lowers the energy to the final level of the catalytic cycle. Overall the free energy profile shows that the reaction is exergonic and suggests carbopalladation as the rate-determining step. A detailed catalytic cycle based on the computational results is shown in Scheme 2.

Ligand Effect. After the reaction energy profile was characterized using L3 as ligand, the effect on the reaction energy profile from the rest of the ligands L1–L7 was investigated, and the results are presented in Figure 5. The relative energies of the presented complexes are shown in Table 2. Complex II was identified as the lowest energy minima preceding decarboxylation for all ligands. The cationic complex III showed a clear trend in relative free energy, where the ligands with methyl substituents (L3, L4, L6, and L7) gave complexes lower in energy in comparison to ligands devoid of methyl substituents (L1, L2, and L5). This trend can be explained by the release of steric crowding in complex II for L3, L4, L6, and L7, in agreement with investigations by others.^{26,34} However, this effect was reduced when progressing to complex IV. Overall, the free energy required for the decarboxylation process from complex II to the transition state TS-I varied in the range $109\text{--}120 \text{ kJ mol}^{-1}$.

Scheme 2. Detailed Catalytic Cycle Based on the Computational Results

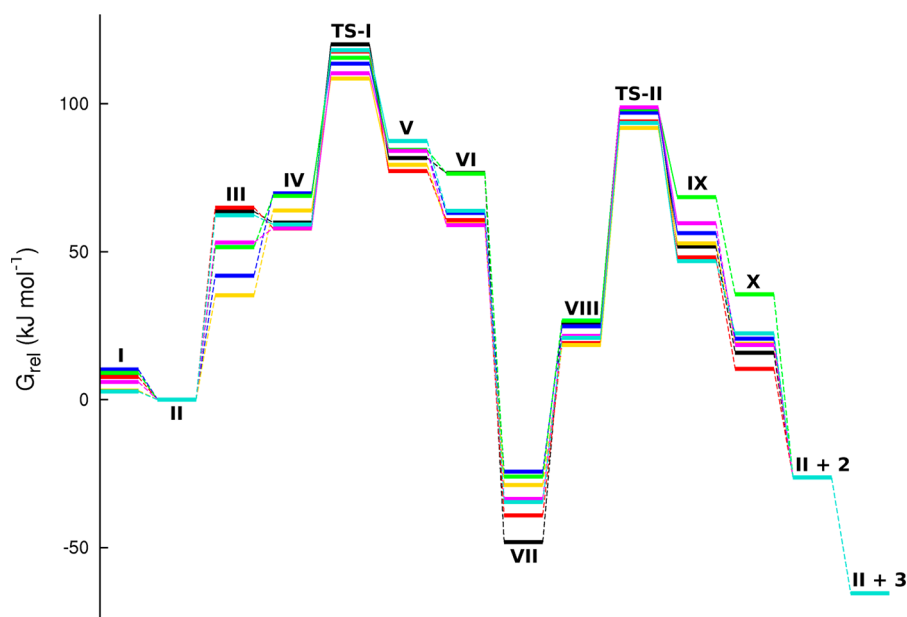
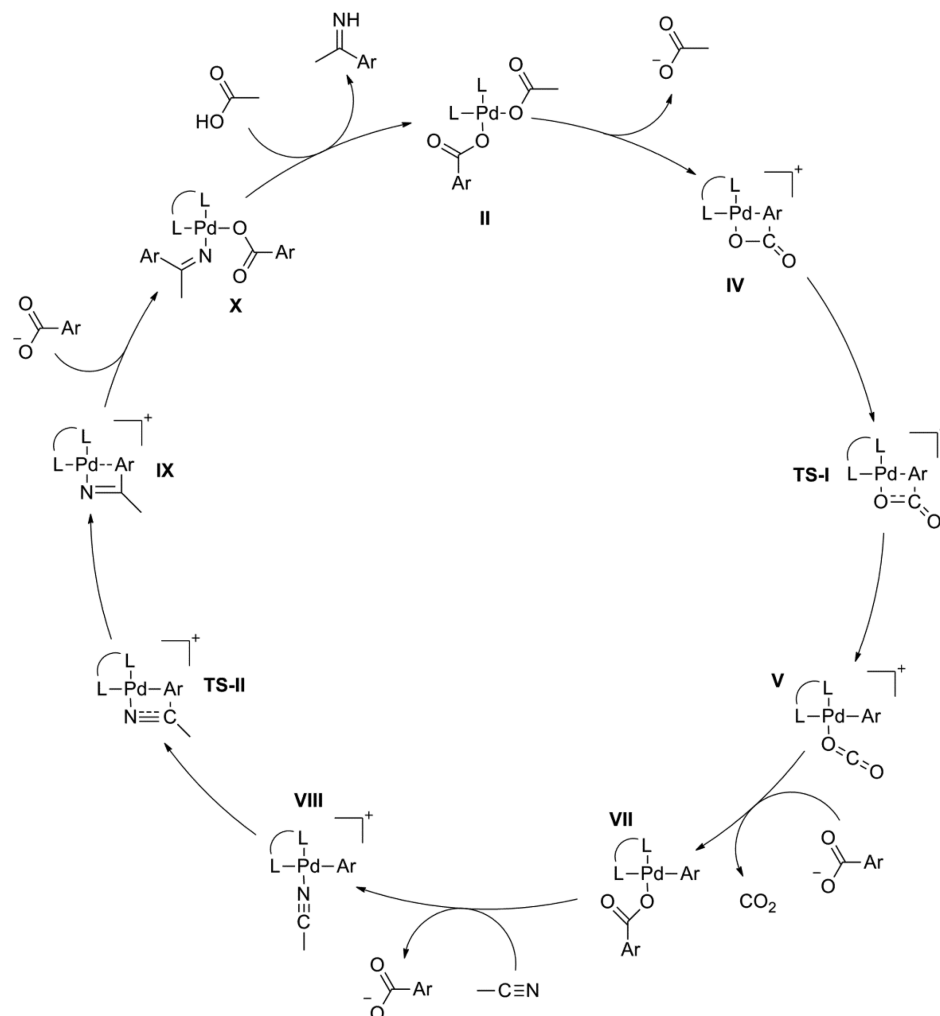


Figure 5. Free energy profile of Pd(II)-catalyzed decarboxylative addition of 2,6-dimethoxybenzoic acid to MeCN for different nitrogen-based ligands (Table 1): L1, black; L2, turquoise; L3, magenta; L4, gold; L5, red; L6, blue; L7, green. Complex structures are the same as in Figures 1 and 2, with the exception that in the low-energy path for L4, L6, and L7 2,6-dimethoxybenzoic acid in complex X has been replaced with acetate.

Table 2. Relative Energies (kJ mol^{-1}) of the Investigated Complexes for All Ligands

	L1	L2	L3	L4	L5	L6	L7
I	9	3	6	3	8	10	9
II	0	0	0	0	0	0	0
III	64	62	53	35	65	42	52
IV	60	59	58	64	58	70	69
TS-I	120	118	110	109	118	114	116
V	82	87	84	79	77	84	84
VI	77	64	59	59	61	63	76
VII	-48	-35	-34	-29	-39	-24	-26
VIII	26	21	22	18	19	25	27
TS-II	99	94	99	92	94	97	98
IX	52	47	60	53	48	56	68
X	16	22	18	19	10	21	36
II + 2	-26	-26	-26	-26	-26	-26	-26
II + 3	-66	-66	-66	-66	-66	-66	-66
$\Delta G_{\text{decarboxylation}}$	120	118	110	109	118	114	116
$\Delta G_{\text{carbopalladation}}$	147	128	132	121	133	121	124

Following TS-I the neutral complex VII was identified as the lowest energy complex for all ligands and, thus, the starting point for carbopalladation. The ligand effect was found to be significant in this complex, and L1 gave a significantly more stable neutral complex in comparison to L3 and L4, which is in line with the lack of sterically demanding methyl groups. The same effect was seen with L2 and L5, albeit not as pronounced. The required energy for carbopalladation was calculated to be in the range $121\text{--}147 \text{ kJ mol}^{-1}$ and was calculated to be the rate-determining catalytic step for all investigated ligands. Overall the free energy required for carbopalladation, with the exception of L3, seems to follow a trend where the higher yielding ligands result in lower required energies for this reaction step. Notably this trend is true also for the decarboxylation, suggesting that both parts of the reaction are favored by the same ligand features. These results suggest that

this method may be used to predict the efficacy of related bidentate, nitrogen-based ligands such as BIAN-type ligands⁵⁰ or bipyridine- and phenanthroline-based ligands with substituents other than methyl to induce steric hindrance and destabilize the neutral square-planar Pd(II) complexes.⁵¹ Thus, ligands perhaps even more efficient than those considered in this work could be identified.

Solvent Effect. In the calculated reaction route, the lowest energy minima preceding both decarboxylation and carbopalladation are neutral complexes, while the respective TSs are cationic. Such charge separation should be facilitated in polar solvents. Although a polar reaction medium using the reactant acetonitrile as solvent was used, the reaction should be further facilitated by using a solvent with increased dielectric constant. This was investigated by calculating the reaction profile using water as solvent. Since L1 was calculated to have the highest energy requirements, this ligand was used when calculating the effect from the solvent on the free energy profile.

A comparison of the reaction profiles using acetonitrile ($\epsilon = 37.5$) and water ($\epsilon = 80.37$)⁵² is shown in Figure 6. As expected, the energy required for both decarboxylation and carbopalladation were calculated to be lower when replacing acetonitrile with the more polar solvent water in the solvation model. The cationic complexes, including the TSs, are stabilized relative to the neutral complexes, which resulted in a reduced energy requirement for decarboxylation and carbopalladation by 23 and 34 kJ mol^{-1} , respectively. Although the energies for both TSs relative to the lowest preceding complex are reduced, carbopalladation is still 26 kJ mol^{-1} higher in energy, which should provide confidence that carbopalladation is the more energetically demanding catalytic step of the two.

The results from the theoretical investigation suggest that the solvent has a large effect on the transformation. From these results we hypothesized that the poor experimental result when employing L1 as ligand in the original reaction protocol could

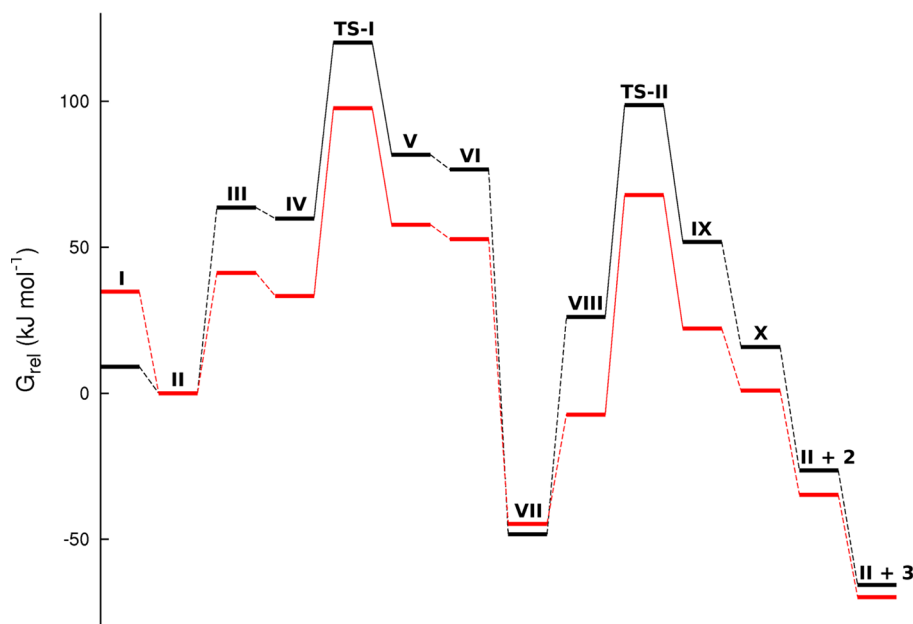


Figure 6. Free energy profile for the reaction using different solvents and L1 as ligand. The black line represents the energy using acetonitrile as reaction media, and the red line represents that using water. Complex structures are the same as in Figures 1 and 2, with the exception that, when using water as solvent, acetate in complex II has been replaced with deprotonated 1 in the low-energy path.

be the high energy requirement for carbopalladation (Table 1 and Figure 5) and that performing the process in solvent systems with increased water concentration would be beneficial under those reaction conditions.

In order to test this hypothesis and to support the calculations, an experimental investigation was performed with L1 as ligand in which the water concentration was varied. First, the effect on yield was investigated by performing four reactions with increasing concentrations of water corresponding to an increasing water/acetonitrile ratio in the reaction vessel, shown in Table 3. The results show a clear trend of increasing yield with increased concentration of water up to 49% yield, which is a yield 3 times higher than that of the original protocol.

Table 3. Effect of Increased Water Concentrations on the Yield of the Reaction

entry	amt of H ₂ O (μL)	yield (%) ^a
1	200	15
2	600	27
3	1100	34
4	1600	49

^aIsolated yields.

Furthermore, the predicted lower energy requirement of the rate-determining carbopalladation when using water as solvent should correspond to an increased reaction rate. This led us to conduct a basic kinetics experiment, measuring the conversion into product over time using two different reaction setups with different amounts of water in the reaction media. For this experiment the two extremes from Table 3, entries 1 and 4, were selected and the total process time divided into six time points. See the Supporting Information for experimental details. The results are shown in Figure 7. The normalized GC-MS response is plotted against reaction time, not including time for heating to the desired temperature. Thus, the higher concentration of product after 5 min for the reaction carried out in a lower water concentration can possibly be attributed to the longer heating time before reaching the set point of that

reaction media as well as the limited solubility of the benzoic acid at lower temperatures in more aqueous solutions. After this initial point, however, the reaction with higher water concentration clearly proceeded at a higher rate than the other, which supports a reduced energy requirement in the rate-determining step.

CONCLUSIONS

In summary, palladium(II)-catalyzed decarboxylative addition of 2,6-dimethoxybenzoic acid to acetonitrile was investigated by means of DFT calculations. The results suggest that carbopalladation is the rate-determining step of the reaction. The beneficial effect from the methyl groups in dimethylated ligands was attributed to destabilization of the neutral square-planar complexes preceding the decarboxylation and carbopalladation TSs, with a more marked effect in the latter reaction step. A significant solvent effect was seen in the calculations, which predicted reduced energy requirements for both decarboxylation and carbopalladation in water and experimental investigations were performed to support the calculations. The experimental results show that increased concentration of water indeed increases the effectiveness and rate of the reaction when employing 2,2'-bipyridine and thus partially reduces the dependency on steric destabilization from the ligands in the reaction.

ASSOCIATED CONTENT

Supporting Information

Text, figures, and tables giving geometries and energies of the presented complexes, experimental procedures for synthesis and kinetic studies, and heating profiles. This material is available free of charge via the Internet at <http://pubs.acs.org>.

AUTHOR INFORMATION

Corresponding Author

*E-mail: Christian.Skold@orgfarm.uu.se

Notes

The authors declare no competing financial interest.

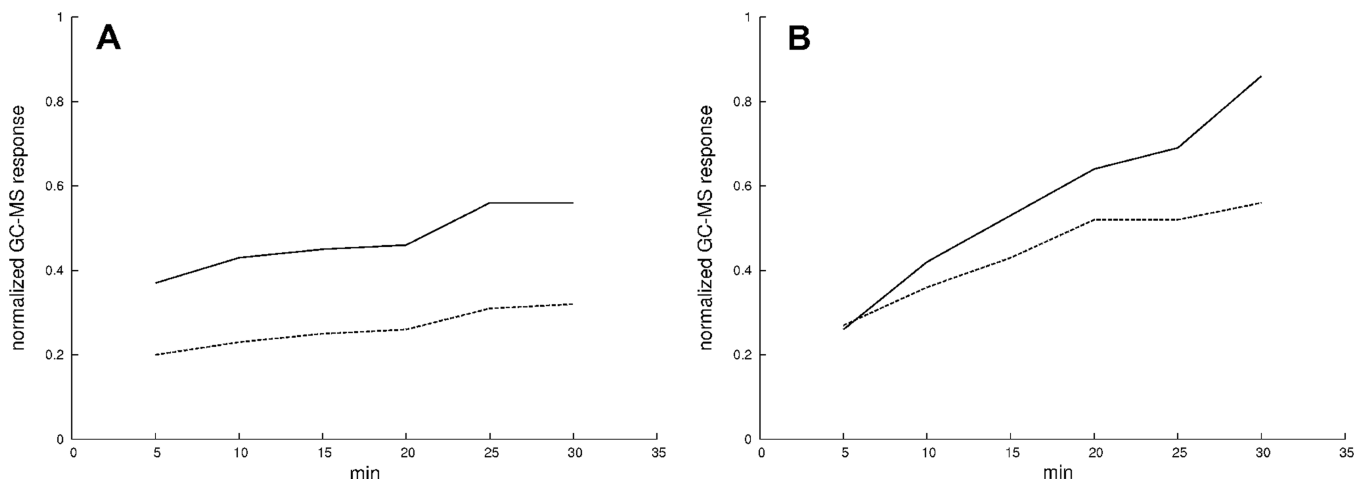


Figure 7. Results from the kinetic study of the reaction using different amounts of water, 200 μL (Table 2, entry 1) in plot A and 1600 μL (Table 2, entry 4) in plot B, at 130 °C for 5, 10, 15, 20, 25, and 30 min, respectively. The GC-MS response is normalized with the response of the internal standard (2-methylnaphthalene, IS) plotted against time (heating time not included). The desired methyl ketone is denoted by solid lines and the decarboxylated byproduct 1,3-dimethoxybenzene by dotted lines.

■ ACKNOWLEDGMENTS

We thank Prof. Per-Ola Norrby and Dr. Luke Odell for fruitful discussions and Dr. Wesley Schaal for linguistic revision. M.L. and R.S.M. are grateful to Erasmus Mundus (EXPERTS Programme) for a Postdoctorate Fellowship. M.L. thanks the Swedish Research Council.

■ REFERENCES

- (1) Garves, K. J. *Org. Chem.* **1970**, *35*, 3273–3275.
- (2) Zhou, C.; Larock, R. C. *J. Am. Chem. Soc.* **2004**, *126*, 2302–2303.
- (3) Zhou, C.; Larock, R. C. *J. Org. Chem.* **2006**, *71*, 3551–3558.
- (4) Hsieh, J.-C.; Chen, Y.-C.; Cheng, A.-Y.; Tseng, H.-C. *Org. Lett.* **2012**, *14*, 1282–1285.
- (5) Goossen, L. J.; Rudolph, F.; Oppel, C.; Rodríguez, N. *Angew. Chem., Int. Ed.* **2008**, *47*, 3043–3045.
- (6) Ueura, K.; Miyamura, S.; Satoh, T.; Miura, M. *J. Organomet. Chem.* **2006**, *691*, 2821–2826.
- (7) Wong, Y.-C.; Parthasarathy, K.; Cheng, C.-H. *Org. Lett.* **2010**, *12*, 1736–1739.
- (8) Zhao, B.; Lu, X. *Tetrahedron Lett.* **2006**, *47*, 6765–6768.
- (9) Lindh, J.; Sjöberg, P. J. R.; Larhed, M. *Angew. Chem., Int. Ed.* **2010**, *49*, 7733–7737.
- (10) Behrends, M.; Sävmarker, J.; Sjöberg, P. J. R.; Larhed, M. *ACS Catal.* **2011**, *1*, 1455–1459.
- (11) Liu, J.; Zhou, X.; Rao, H.; Xiao, F.; Li, C.-J.; Deng, G.-J. *Chem. Eur. J.* **2011**, *17*, 7996–7999.
- (12) Miao, T.; Wang, G.-W. *Chem. Commun.* **2011**, *47*, 9501–9503.
- (13) Rodríguez, N.; Goossen, L. J. *Chem. Soc. Rev.* **2011**, *40*, 5030–5048.
- (14) Smith, M. B.; March, J. *March's Advanced Organic Chemistry: Reactions, Mechanisms, and Structure*. 6th ed.; Wiley: Hoboken, NJ, 2007; pp 745–747.
- (15) Gooßen, L. J.; Deng, G.; Levy, L. M. *Science* **2006**, *313*, 662–664.
- (16) Gooßen, L. J.; Thiel, W. R.; Rodríguez, N.; Linder, C.; Melzer, B. *Adv. Synth. Catal.* **2007**, *349*, 2241–2246.
- (17) Dickstein, J. S.; Mulrooney, C. A.; O'Brien, E. M.; Morgan, B. J.; Kozłowski, M. C. *Org. Lett.* **2007**, *9*, 2441–2444.
- (18) Goossen, L. J.; Linder, C.; Rodríguez, N.; Lange, P. P.; Fromm, A. *Chem. Commun.* **2009**, 7173–7175.
- (19) Dupuy, S.; Lazreg, F.; Slawin, A. M. Z.; Cazin, C. S. J.; Nolan, S. P. *Chem. Commun.* **2011**, *47*, 5455–5457.
- (20) Sun, Z.-M.; Zhang, J.; Zhao, P. *Org. Lett.* **2010**, *12*, 992–995.
- (21) Gooßen, L. J.; Zimmermann, B.; Knauber, T. *Angew. Chem., Int. Ed.* **2008**, *47*, 7103–7106.
- (22) Gooßen, L. J.; Zimmermann, B.; Knauber, T. *Angew. Chem.* **2008**, *120*, 7211–7214.
- (23) Gooßen, L. J.; Rodríguez, N.; Lange, P. P.; Linder, C. *Angew. Chem.* **2010**, *122*, 1129–1132.
- (24) Goossen, L. J.; Rodríguez, N.; Melzer, B.; Linder, C.; Deng, G.; Levy, L. M. *J. Am. Chem. Soc.* **2007**, *129*, 4824–4833.
- (25) Goossen, L. J.; Rodríguez, N.; Lange, P. P.; Linder, C. *Angew. Chem., Int. Ed.* **2010**, *49*, 1111–1114.
- (26) Xue, L.; Su, W.; Lin, Z. *Dalton Trans.* **2010**, *39*, 9815–9822.
- (27) Zhang, S.-L.; Fu, Y.; Shang, R.; Guo, Q.-X.; Liu, L. *J. Am. Chem. Soc.* **2009**, *132*, 638–646.
- (28) Sraji, L. O. C.; Khairallah, G. N.; da Silva, G.; O'Hair, R. A. J. *Organometallics* **2012**, *31*, 1801–1807.
- (29) Chuchev, K.; BelBruno, J. J. *J. Mol. Struct. (THEOCHEM)* **2007**, *807*, 1–9.
- (30) Ruelle, P. *J. Chem. Soc., Perkin Trans. 2* **1986**, 1953–1959.
- (31) Li, J.; Brill, T. B. *J. Phys. Chem. A* **2003**, *107*, 2667–2673.
- (32) Ruelle, P. *J. Comput. Chem.* **1987**, *8*, 158–169.
- (33) Shi, J.; Huang, X.-Y.; Wang, J.-P.; Li, R. *J. Phys. Chem. A* **2010**, *114*, 6263–6272.
- (34) Hansson, S.; Norrby, P. O.; Sjögren, M. P. T.; Åkermark, B.; Cucciolito, M. E.; Giordano, F.; Vitagliano, A. *Organometallics* **1993**, *12*, 4940–4948.
- (35) Jaguar; Schrödinger LLC, New York, 2011.
- (36) Becke, A. D. *J. Chem. Phys.* **1993**, *98*, 5648–5652.
- (37) Becke, A. D. *J. Chem. Phys.* **1993**, *98*, 1372–1377.
- (38) Lee, C.; Yang, W.; Parr, R. G. *Phys. Rev. B* **1988**, *37*, 785–789.
- (39) Hay, P. J.; Wadt, W. R. *J. Chem. Phys.* **1985**, *82*, 299–310.
- (40) Sousa, S. F.; Fernandes, P. A.; Ramos, M. J. *J. Phys. Chem. A* **2007**, *111*, 10439–10452.
- (41) Ahlquist, M.; Fabrizi, G.; Cacchi, S.; Norrby, P.-O. *J. Am. Chem. Soc.* **2006**, *128*, 12785–12793.
- (42) Henriksen, S. T.; Tanner, D.; Skrydstrup, T.; Norrby, P.-O. *Chem. Eur. J.* **2010**, *16*, 9494–9501.
- (43) Marten, B.; Kim, K.; Cortis, C.; Friesner, R. A.; Murphy, R. B.; Ringnalda, M. N.; Sitkoff, D.; Honig, B. *J. Phys. Chem.* **1996**, *100*, 11775–11788.
- (44) Tannor, D. J.; Marten, B.; Murphy, R.; Friesner, R. A.; Sitkoff, D.; Nicholls, A.; Honig, B.; Ringnalda, M.; Goddard, W. A. *J. Am. Chem. Soc.* **1994**, *116*, 11875–11882.
- (45) Grimme, S.; Antony, J.; Ehrlich, S.; Krieg, H. *J. Chem. Phys.* **2010**, *132*, 154104–19.
- (46) Maroth, S. A. d. *XYZ-viewer, version 0.970*, Stockholm, 2010.
- (47) McMullin, C. L.; Jover, J.; Harvey, J. N.; Fey, N. *Dalton Trans.* **2010**, *39*, 10833–10836.
- (48) Fristrup, P.; Ahlquist, M.; Tanner, D.; Norrby, P.-O. *J. Phys. Chem. A* **2008**, *112*, 12862–12867.
- (49) Ahlquist, M.; Kozuch, S.; Shaik, S.; Tanner, D.; Norrby, P.-O. *Organometallics* **2005**, *25*, 45–47.
- (50) Van Asselt, R.; Elsevier, C. J. *Organometallics* **1992**, *11*, 1999–2001.
- (51) Sjögren, M.; Hansson, S.; Norrby, P. O.; Åkermark, B.; Cucciolito, M. E.; Vitagliano, A. *Organometallics* **1992**, *11*, 3954–3964.
- (52) Values as used in Jaguar 7.8.